Synergic effect of optogenetic stimulation and motor training boosts recovery of motor functionality after stroke supported by segregation of motor representation

Emilia Conti[1,2], Anna Letizia Allegra Mascaro[2,3], Alessandro Scaglione[1], Giuseppe de Vito[2,4], Francesco Calugi[3,4], Maria Pasquini[5,6], Tommaso Pizzorusso[3,4], Silvestro Micera[5,6], Francesco Saverio Pavone[1,2,7]

1 Department of Physics and Astronomy, University of Florence, Italy

2 European Laboratory for Non-linear Spectroscopy University of Florence, Italy

3 Neuroscience Institute, National Research Council, Pisa, Italy

4 Department of Neurofarba, University of Florence, Italy

5 Scuola Superiore Sant'Anna, Pisa, Italy

6 Ecole Polytechnique Federale de Lausanne (EPFL), Lausanne, Switzerland

7 National Institute of Optics, National Research Council, Italy

Keywords

Calcium imaging; photothrombotic stroke; rehabilitation; optogenetic stimulation; motor training; plasticity marker; Schallert test.

Abstract

An ischemic event is followed by extensive changes in cortical excitability involving both hemispheres. Plasticity in the injured hemisphere plays a crucial role in post-stroke motor recovery and is a primary target for rehabilitation therapy. Though stimulation of the ipsilesional motor cortex, especially when paired with motor training, facilitates plasticity and functional restoration, the mechanisms underneath the reshaping of cortical functionality are widely unknown. Here, we designed a protocol of optogenetic stimulation of the peri-infarct region as a neuro-plasticizing treatment coupled with a repetitive motor training. This treatment promoted a generalized recovery in forelimb dexterity and the rescue of the essential features of cortical activation profiles during the execution of the motor training. The present work, by exploiting different approaches, provides a fundamental means to better understand the mechanisms underlying the recovery of motor functionality.

Introduction

Ischemic injuries within the motor cortex result in functional deficits that may profoundly alter the patients' quality of life. Survivors are often chronically impaired in their movements and left with long-term disability (Schwab, 2010). To maximally regain sensory and motor functions after stroke, surviving neural circuits are

reorganized (Dancause and Nudo, 2011; Murphy and Corbett, 2009; Zeiler and Krakauer, 2013). Multiple strategies were developed to enhance neural rewiring and dramatically improve motor outcomes (Zeiler and Krakauer, 2013). These strategies include pharmacological treatment, brain stimulation, and motor training. Among them, stimulation techniques, such as transcranial magnetic stimulation (TMS) and transcranial direct current stimulation (tDCS), represent a promising non-invasive approach to improve cortical remapping. Nevertheless, these treatments can induce diffuse and non-specific activation in mixed neuronal populations (Iwai et al., 2010; Takatsuru et al., 2009; Zhao and Rempe, 2010). With the emergence of optogenetics, targeted neuronal populations could be activated or inhibited achieving a high temporal and spatial precision (Boyden et al., 2005; Li et al., 2016; Yizhar et al., 2011). Indeed, there is a pressing interest in the use of optogenetics to modify the excitatory/inhibitory balance of brain circuits affected by a stroke lesion (Murase et al., 2004; Vallone et al., 2016; Volz et al., 2017).

Previous studies have shown that repeated optogenetic neuronal stimulation of the ipsilesional hemisphere induces a significant improvement in neurovascular coupling response (Cheng et al., 2014). Furthermore, it has been demonstrated that chronic optogenetic stimulation of the entire cortical mantle promotes behavioral recovery associated with the formation of new and stable thalamocortical synaptic boutons (Tennant et al., 2017). Even though large-scale remapping is known to be an important factor in the recovery of lost functionalities (Siegel et al., 2016; Siegel et al., 2018), how the global activity over the ipsilesional hemisphere is redistributed after optogenetic stimulation is still largely unknown.

Furthermore in this framework, motor practice with the paretic limb during the first weeks after stroke improves functional recovery and behaviorally relevant neural repair both in animal models (Biernaskie and Corbett, 2001; Jones et al., 1999; Nudo et al., 1996) and in humans (Butefisch, 2006; Dong et al., 2007; Jaillard et al., 2005; Liepert et al., 2000; Sawaki et al., 2008). Furthermore, in the last years, neurorehabilitation protocols based on the use of robotic devices have shown to provide promising clinical results. The use of robotic devices in murine models and human patients gives an unbiased evaluation of recovery of motor performances providing an accurate description of kinetic and kinematic aspects on motor performance during rehabilitation after stroke (Allegra Mascaro et al., 2019; Balasubramanian et al., 2010; Hogan and Krebs, 2011; Spalletti et al., 2014). Importantly, it is increasingly recognized that the combination of stimulation with physical rehabilitation synergistically creates a pro-plasticizing milieu where spared neurons are more susceptible to experience-dependent modifications (Alia et al., 2017; Straudi et al., 2016; Zeiler and Krakauer, 2013). To our knowledge, no investigation has yet described how the combination of optogenetic stimulation and motor training longitudinally molds cortical functional maps in the chronic phase after stroke.

In the present study, we observe that the combination of ipsilesional optogenetic stimulation and repetitive motor training promotes faster recovery of forelimb functionality compared to optogenetic stimulation only. Furthermore, the rapid behavioral recovery is associated with the segregation of the motor-evoked map of activation and with the restoration of the critical features of calcium profiles. Finally, we found a massive expression of GAP43 in the peri-infarct area and axonal sprouting in the contralesional hemisphere.

Results

Optogenetic rehabilitation of peri-infarct area restores forelimb functionality but not calcium dynamics

We used a photothrombotic stroke model in the primary motor cortex (M1) of the right hemisphere on Thy1-GCaMP6f mice (Figure S1A). We used a 473 nm laser to optogenetically stimulate the peri-infarct area expressing the light-gated cation channel Channelrhodopsin 2 (ChR2) (Figure 1A). The stimulation paradigm lasted four weeks starting 5 days after stroke and consisted of three successive 30-sec laser stimulations, separated by 1-min rest intervals (Figure 1B, top). Stimulation protocol has been calibrated using a laser power right below the one necessary to elicit the forelimb movement and therefore was adjusted over the weeks for each mouse. We divided our sample in three groups (Figure 1B, lower panel): Sham (no stroke), Stroke (stroke, stimulation, no ChR2), Optostim (stroke, stimulation, Chr2). We stimulated Stroke mice not expressing ChR2 to evaluate possible artifacts due to repeated laser stimulation. All the experiments revealed that repeated stimulation did not affect post-stroke recovery. All groups performed at least 5 days of motor training on a robotic device, the M-Platform (Spalletti et al., 2014). The motor training started 25 days after the injury and consisted of 15 cycles of passive extension of the affected forelimb followed by its active retraction triggered by an acoustic cue. We exploited a custom made wide-field microscope (Conti et al., 2019) characterized by a double illumination path to sequentially perform optogenetic stimulation and calcium imaging while the awake mouse performed motor training. We longitudinally tested mice dexterity on the Schallert cylinder test by quantifying the Asymmetry index (A.i.). While spontaneously recovered (Stroke) mice did not reach pre-stroke levels of A.i., a full recovery of forelimb functionality was achieved after four weeks of optogenetic rehabilitation (Optostim, Figure 1C). We then assessed if the behavioral recovery was associated with alteration in motor-evoked cortical functionality. Evaluation of motor-evoked cortical activity was investigated during motor training by performing wide-field calcium imaging on the affected hemisphere of GCaMP6f mice. We aimed to characterize the activation maps and the critical features of calcium transient, with a focus on the analysis of those transients occurring in the time-window of the retraction movement (Figure 1D, S1B). We first analyzed the spatial extension of the motor representation by overlapping the movement-triggered activation maps obtained for each day of training. By comparing the maps of activation in the three experimental groups we observed a segregated activation in healthy mice while in Stroke and Optostim mice the map covered most of the affected hemisphere (Figure 1E). By analyzing the fluorescence signal in the region of maximum activation, we observed that in terms of amplitude and timing, the calcium activation of Optostim group did not recover the features of healthy animals (Figure 1F, G). These combined results demonstrate that even though recovery of forelimb dexterity can be achieved by optogenetic stimulation, the corresponding motor-evoked calcium activation was dissimilar in spatiotemporal terms to the healthy mice.

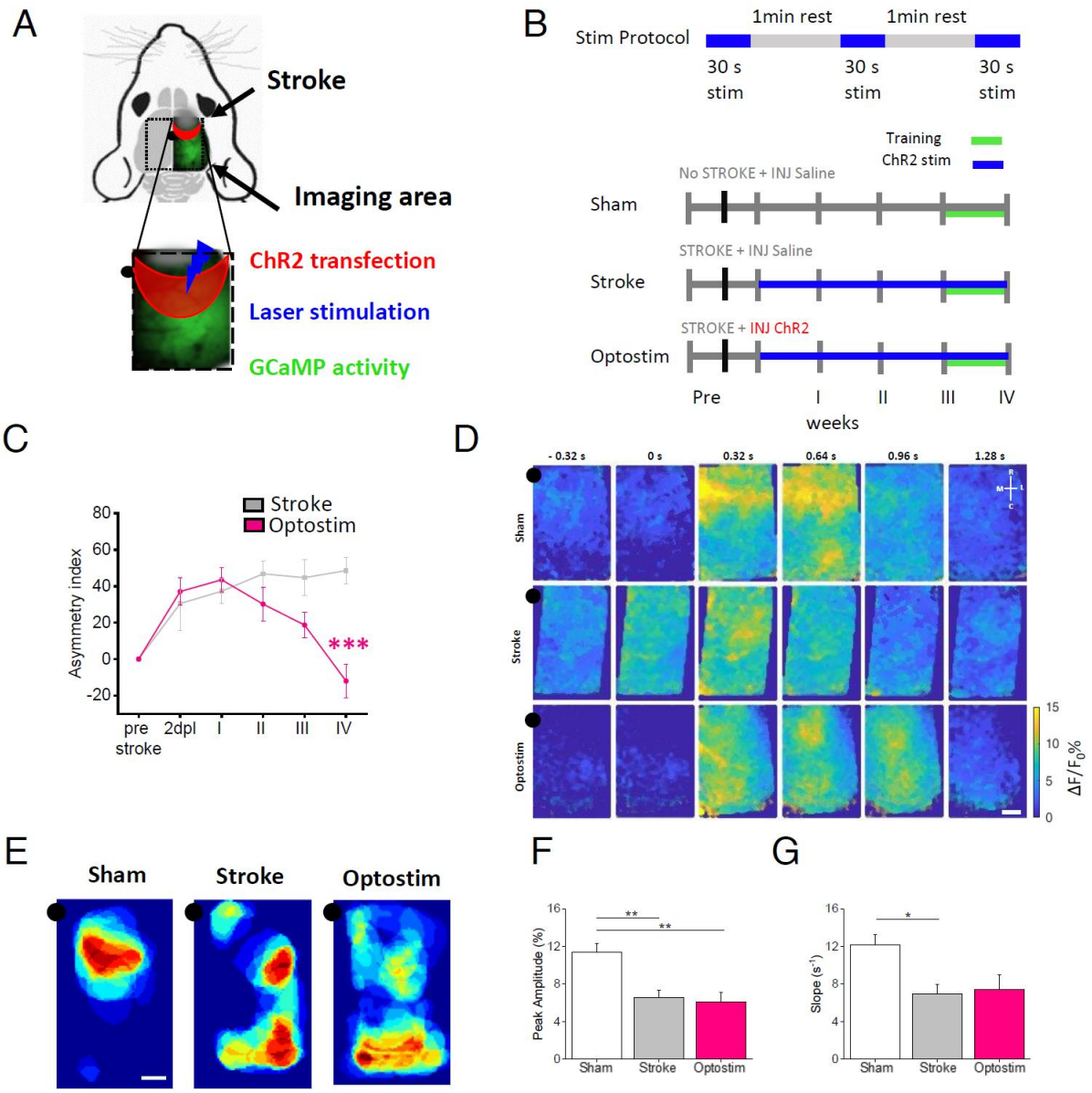

Figure 1. Optogenetic stimulation of peri-infarct area: (A) Schematic representation of field of view for optogenetic stimulation: ChR2-expressing neurons (area in red) are stimulated by a blue laser. Cortical activity is revealed in the right hemisphere during the motor training. The grey cloud represents the stroke core, the black dot represents bregma. (B) Top: stimulation paradigm consisting of 3 stimulation train (5Hz, 10 msec) separated by 1-minute rest intervals. Bottom: experimental timeline for Sham, Stroke and Optostim groups. (C) Asymmetry index analysis for Optostim group (in pink) compared to non-rehabilitated animals (Stroke group in grey); two-way Anova repeated measure followed by Bonferroni's test: $p<0,0001$. (D) Image sequence of cortical activation as assessed by calcium imaging during pulling of contralateral forelimb, from 0.32 s before to 1.28 s after the onset of the force peak. Each row shows a representative sequence from a single animal of each group. Black dot represents the bregma. Scale bar 1 mm. (E) The panels show the average thresholded region of maximum activation trigger by the pulling task for each experimental group. The black dot represents the bregma. Scale bar 1 mm. (F) Graph shows the maximum of fluorescence peaks

(average ± SEM) of calcium transient (Peak Amplitude_Sham = 11.4 ± 0.9 %; Peak Amplitude_Stroke = 6.6 ± 0.7%; Peak Amplitude_Optostim = 6.1 ± 0.9%; one-way ANOVA followed by Tukey's test: pSham-Stroke= 0.007; pSham-Optostim =0.003). (G) Graph shows the Slope (average ± SEM) of the fluorescence in the rising phase of the trace (Slope_Sham = 12.1 ± 1.1 s^{-1}; Slope_Stroke = 6.9 ± 1.0 s^{-1}, Slope_Optostim = 7.4 ± 1.5 s^{-1}; one-way Anova followed by Tukey's test: pSham-Stroke = 0.04). nSham=3; nStroke=4; nOptostim=4.

A novel rehabilitation paradigm combines optogenetic stimulation with motor training

We then guessed if a more effective recovery could be achieved by coupling the same optogenetic stimulation protocol to repetitive motor training of the contralesional forelimb. We, therefore, examined the consequences of combined optogenetic stimulation and motor training (OR group) and compared it to motor exercise alone (Robot group). Mice started training on the M-Platform during the acute phase after stroke (Figure 2A-B). Robot mice performed four weeks of motor rehabilitation starting 5 days after stroke. In addition to the same physical exercise, OR mice were exposed to daily optogenetic stimulation of the perilesional cortex along four weeks (Figure 2B). By analyzing the force traces associated with the active pulling of the contralesional forelimb we observed a progressive modulation of the force peaks in amplitude (Peak Prominence), in width (Full-Width Half Maximum, FWHM) and training duration during motor training in OR animals (Figure 2C). In detail, a significant reduction in the force peak width is observed at the end of the rehabilitative period in OR mice compared to spontaneously recovered (Stroke) mice. This improvement is likely attributable to the training on the platform itself since the motor rehabilitation alone (Robot group) induces a similar trend in the force peaks (Figure S1D). In detail, the progressive reduction of the Time to target visible in double-treated mice is in line with previous findings in robot-treated stroke mice (Spalletti et al., 2014). We then evaluated through behavioral analysis (Schallert test) alterations in spontaneous forelimbs use. In accordance with Spalletti et al., 2017 (Spalletti et al., 2017), motor training alone was not enough to restore per-stroke performances (Figure S1E). Conversely, OR mice achieved excellent results in forelimb dexterity as early as the second week of rehabilitation compared to spontaneously recovered mice (Stroke group) (Figure 2D).

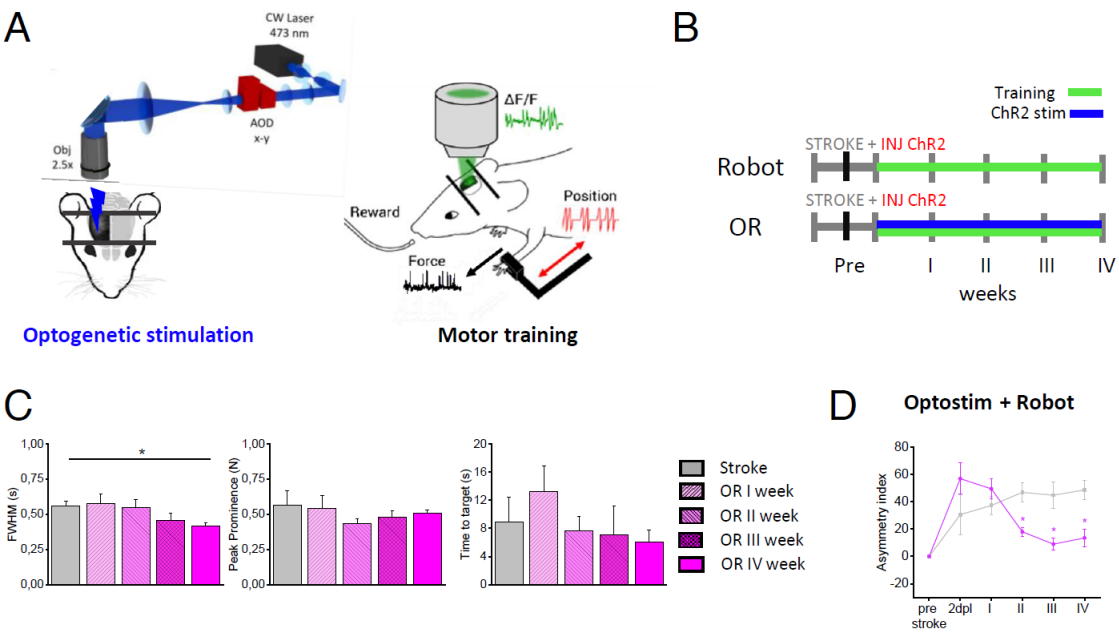

Figure 2. A novel rehabilitation paradigm combines optogenetic stimulation with motor training: (A) Graphical representation of combined rehabilitative protocol: on the left a sketch of laser path for optogenetic stimulation; on the right a cartoon of the M-Platform used for motor training. (B) Experimental timeline for Robot and OR groups. (C) Force analysis during pulling task (average ± SEM). Left panel shows Full Width Half Maximum of the force peak (Stroke= 0,56 ± 0,03; OR_Iweek= 0,57 ± 0,07; OR_IIweek= 0,55 ± 0,06; OR_IIIweek= 0,45 ± 0,05; OR_IVweek= 0,42 ± 0,02; t-test: pStroke-OR_IVweek= 0,03). Middle panel shows Peak Prominence (Stroke= 0,56 ± 0,10; OR_Iweek= 0,54 ± 0,09; OR_IIweek= 0,43 ± 0,03; OR_IIIweek= 0,48 ± 0,04; OR_IVweek= 0,51 ± 0,02). Right panel shows Time to Target (Stroke= 8,8 ± 3,6; OR_Iweek= 13,2 ± 3,6; OR_IIweek= 7,6 ± 2,1; OR_IIIweek= 7,1 ± 4,1; OR_IVweek= 6,0± 1,8). (D) Asymmetry index analysis of OR (in violet) mice compared to non-rehabilitated animals (Stroke group in grey); two-way Anova repeated measure followed by Bonferroni's test: p-weekII=0,005; p-weekIII=0,0004; p-weekIV=0,0006. nStroke=4; nOR=4.

Combined rehabilitation recovers motor-evoked cortical activation profiles

Considering the faster functional improvement induced by combined rehabilitation compared to optogenetic stimulation alone, we wondered if the behavior mirrored different patterns of motor-evoked cortical activity. To this aim, we assessed the cortical activation in the affected hemisphere while the awake animals performed the motor training on the M-Platform. Wide-field calcium imaging showed that calcium activation maps of both Robot and OR groups was comparable to healthy controls (Sham) in terms of extension, meaning that daily motor training promotes the refocusing of the cortical motor output four weeks after stroke (Figure 3A, B). More in detail, the cortical maps obtained for the Robot group appeared to be shifted towards sensory areas with respect to Sham mice. Furthermore, the maps of activation of OR mice appeared to be more medial with respect to that of healthy mice, suggesting that during the last week of rehabilitation, the principal region of the cortex activated during contralateral forelimb pulling was the secondary motor cortex. To verify if these

features in motor representation maps were associated with different patterns of propagation of calcium activity, we analyzed the temporal profile of calcium transients in the region of movement-triggered maximal activation. After classifying the calcium peaks based on the kinematic and dynamic data measured on the M-Platform, we reconstructed the calcium dynamic during force application by the injured forelimb. By comparing the peak amplitude and slope of healthy animals (Sham), non-rehabilitated mice (Stroke), Robot and OR groups, we observed that single treatment with M-Platform was not sufficient to induce a full recovery to pre-stroke levels. On the other hand, the synergic effect of combined rehabilitation promoted the reestablishment of these salient features of calcium transient in the peri-infarct area (Figure 3C, D). Longitudinal calcium imaging showed a positive trend for OR mice compared to Robot group starting from the second week of rehabilitation (Figure S1C). The pronounced increment in Peak amplitude and Slope of calcium transient in combined rehabilitated mice became comparable to values distinctive of health condition after four weeks of combined treatment.

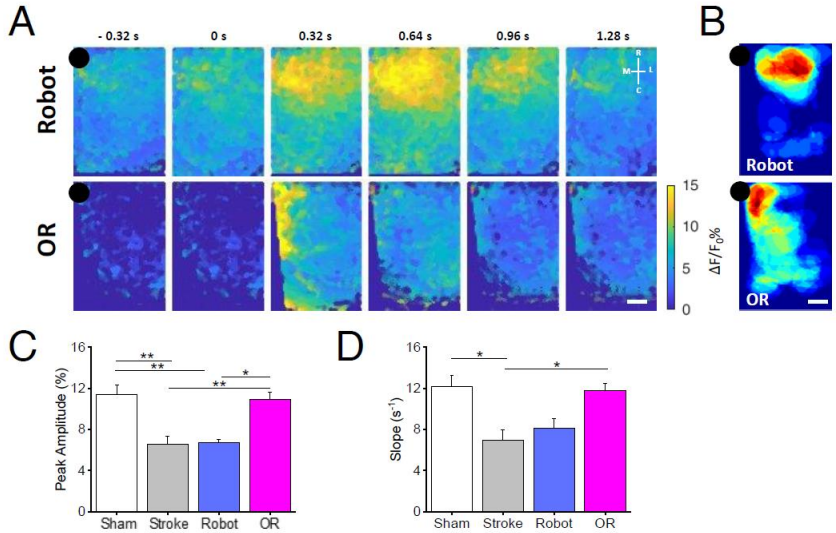

Figure 3. Combined rehabilitation restores functional connectivity: (A) Image sequence of cortical activation as assessed by calcium imaging during pulling of the handle by the contralateral forelimb, from 0.32 s before to 1.28 s after the onset of the force peak. Each row shows a representative sequence from a single animal of each group. Black dot represents the bregma. Scale bar 1 mm. (B) The panels show the average thresholded ROI computed for each experimental group. The black dot represents the bregma. Scale bar 1 mm. (C) Graph shows the maximum of fluorescence peaks (average ± SEM) of calcium transient (Peak Amplitude_Sham = 11.4 ± 0.9 %; Peak Amplitude_Stroke = 6.6 ± 0.7%; Peak Amplitude_Robot = 6.7 ± 0.3%; Peak Amplitude_OR = 10.9 ± 0.7%; one-way ANOVA followed by Tukey's test: pSham-Robot = 0.01; pStroke-OR = 0.009; pRobot-OR=0.02). (D) Graph shows the slope (average ± SEM) of the fluorescence in the rising phase of the trace 14 (Slope_Sham = 12.1 ± 1.1 s^{-1}; Slope_Stroke = 6.9 ± 2.0 s^{-1}, Slope_Robot = 8.1 ± 0.9 s^{-1}; Slope_OR = 11.8 ± 0.7 s^{-1}; one-way Anova followed by Tukey's test: pStroke-OR = 0.04); nSham=3; nStroke=4; nRobot=3; nOR=4.

Immunohistochemical evaluation in the peri-infarct area

To identify potential mechanisms underlying recovery, we carried out an immunohistochemical analysis of plasticity indicators in the peri-infarct cortex of all experimental groups at the end of the rehabilitation period, 30 days after the lesion. First, we examined the expression of the growth-associated protein 43 (GAP43), a plasticity marker involved in synaptic turnover and reorganization after stroke (Carmichael, 2003; Carmichael et al., 2005; Murphy and Corbett, 2009). While with optogenetic stimulation or motor training GAP43 expression levels were comparable to spontaneously recovered mice, the combined rehabilitative treatment promoted a massive expression of this neuronal plasticity marker (Figure 4A, Figure S2A). This boost was localized to the peri-infarct area since GAP43 expression in the contralesional hemisphere was not significantly different between the groups. By analyzing the homotopic areas in the contralesional hemisphere, we revealed in Optostim, Robot and OR mice an increase in number and length of axonal projections (Figure 4B, Figure S2A right panel) compared to Stroke mice where GAP43+ fibers were very infrequent. This suggested that both perilesional stimulation and motor training enhance the axonal sprouting in distal regions functionally related to the stroke core. Moreover, the combinatorial treatment further boosts the plasticity towards the contralesional hemisphere.

The excitatory/inhibitory balance is known to be profoundly altered by stroke (Jones and Atkins 2015). Rehabilitation treatments possibly recover the equilibrium by shaping cortical excitability (Cheng et al., 2014). To test this hypothesis, we evaluated the density of parvalbumin-positive cells (PV+) in the peri-infarct region. We observed a significative increase of PV+ cells in OR mice compared to non-treated animals. Single treatments were not able to induce a similar level of PV expression (Figure 4C, S2B). Together with the increased motor-evoked activation levels in pyramidal cells, the synergic effect of combined rehabilitation could promote the establishment of a new excitatory/inhibitory equilibrium in the peri-infarct and contralesional hemispheres. Finally, to scrutinize the involvement of neuroprotective factors, we analyzed if the combined treatment altered the expression levels of miR-29 in the peri-infarct cortex four weeks after the lesion. We observed an upregulation of miR-29 expression in OR mice compared to spontaneously recovered mice (Figure S2C).

Taken together, the histological analysis show that behavioral and functional improvements after combined rehabilitation are supported by an increased expression of both plasticizing and neuroprotective factors.

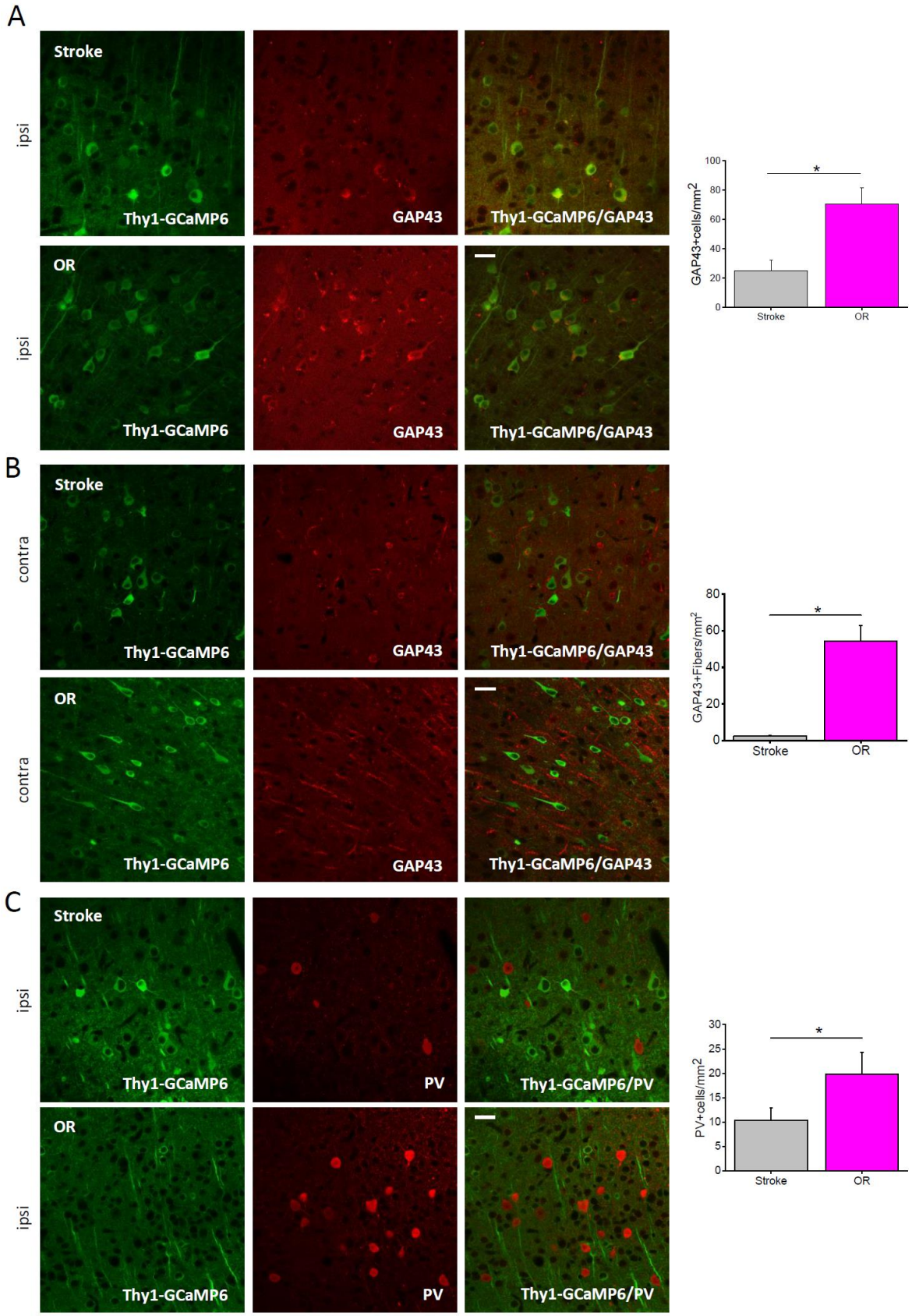

Figure 4. Immunohistochemical evaluation in the peri-infarct area: (A) Left: Transgenic expression of GCaMP6f under Thy1 promoter (in green) and representative GAP43 immunostaining (in red) of a coronal section (100 µm thick) of a Stroke and OR mouse. Right: Quantification of GAP43+ cells in the peri-infarct

area for Stroke and OR groups (Stroke= 25,0 ± 7,2; OR= 70,7 ± 10,7; one-way ANOVA followed by Fisher's test: pStroke-OR= 0,011). (B) Left: transgenic expression of GCaMP6f indicator under Thy1 promoter (in green) and representative GAP43 immunostaining (in red) of GAP43+ fibers in the contralesional hemisphere. Right: Quantification of GAP43+ fibers in the contralesional hemisphere for Stroke and OR mouse (Stroke= 2,4 ± 0,4; OR= 54,4 ± 8,3; one-way ANOVA followed by Bonferroni's test: pStroke-OR= 0,006); nStroke=4; nOptostim=4; nRobot=3; nOR=4. (C) Left: transgenic expression of GCaMP6f indicator under Thy1 promoter (in green) and representative PV immunostaining (in red) of a Stroke and OR mouse. Right: Quantification of PV+ cells for Stroke and OR groups in the peri-infarct area (Stroke= 19,7 ± 5,0; OR= 37,7 ± 8,3; one-way ANOVA followed by Fisher's test: pStroke-OR= 0,04). Scale bar 20 µm.

Discussion

In the present study, we assessed the cortical alterations induced by optogenetic stimulation of the ipsilesional hemisphere alone and in combination with motor rehabilitation in a mouse model of stroke in the primary motor cortex. We first evaluated the effect of four weeks of repeated stimulation of the ipsilesional cortex. In agreement with a previous work by Tennant and collaborators (Tennant et al., 2017) showing that optogenetic stimulation of thalamocortical axons over the entire dorsal cortex enhances the recovery of forepaw sensorimotor abilities, we found that four weeks of optogenetic stimulation targeted to ChR2-transfected perilesional cortex leads to a remarkable motor improvement. Nevertheless, our observations indicate that this treatment *per se* does not recover pre-stroke features of motor-evoked cortical activation. Indeed, a less segregated activation involving almost the entire lesioned hemisphere is observed. The dissociation between behavioral and mesoscale cortical functionality was previously described by Balbi and colleagues in a recent work (Balbi et al., 2018), where post-stroke behavioral impairment was not associated to alterations in functional connectivity. In our study, a possible explanation for behavioral/cortical activity dissociation might lay in the intervention of the contralesional hemisphere. In the acute phase after stroke, increases in contralesional M1 excitability may result in an excessive inhibitory effect on the ipsilesional cortex, which may interfere with its reorganization (Buetefisch, 2015; Butefisch et al., 2008; Murase et al., 2004; Shimizu et al., 2002). Under the hypothesis that optogenetic stimulation of the peri-infarct excitatory neurons counteracts this inhibitory drive by hyper-activating the spared neurons, the recovery of forelimb dexterity might be supported by a new excitatory/inhibitory balance between the two hemispheres. This is in agreement with our previous work (Allegra Mascaro et al., 2019) showing that the transient silencing of the homotopic motor cortex was necessary to achieve a generalized recovery. The present study confirms this hypothesis, since stimulating the perilesional neurons might counterbalance the contralesional inhibitory inference and eventually lead to an adaptive recovery of forelimb functionality. Further investigations on the contralesional cortical activity will address this hypothesis.

Conversely, Robot mice during the four weeks of treatment improved their performance on M-Platform, but motor training alone was not sufficient to promote a generalized recovery in a different motor task. Nevertheless, repetitive motor training results in higher spatial segregation of the motor-evoked cortical maps

of activation. This result suggests that motor training alone promotes task-specific remodeling of cortical connectivity.

Finally, the combined rehabilitative treatment triggers a synergic effect that embraces both behavioral and functional spheres. Indeed, asymmetry index analysis indicated that the combination of these two strategies induces a faster restoration of the forelimb functionality as measured in the Schallert test, towards healthy conditions. Indeed, forelimb dexterity was restored to pre-stroke levels already at the end of the second week of combined rehabilitation, two weeks before the optostimulation-treated mice. At the same time flanking the stimulation with repeated exercise promoted both behavioral improvement and progressive segregation of motor-associated circuitry in the peri-lesioned cortex.

The behavioral improvement is supported by the long-lasting expression of growth-associated factors in the perilesional area, as demonstrated by the increased number of $GAP43^{+}$ cells. This factor is known to promote both cortical remapping (Murphy and Corbett, 2009) and axonal sprouting (Carmichael, 2003; Carmichael et al., 2005; Murphy and Corbett, 2009) after stroke. Accordingly, we see an increase in motor-evoked cortical activation in parallel with segregation mediated by excitatory cells in the peri-infarct area of OR mice compared to spontaneous and single treatments. Together with the higher levels of parvalbumin expression, these results suggest that the combined treatment might promote the restoration of excitatory/inhibitory balance in the peri-infarct cortex.

The recovery of the excitatory/inhibitory balance appears to be further supported by the sprouting of axons in the contralesional cortex, where a substantial number of GAP43+ fibers were detected. In addition, results show a modest increase in miR-29 expression following optical stimulation. Considering the role of miR-29 in modulating the cellular responses required for counteracting ischemic insult (Kobayashi et al., 2019), our data reinforce the hypothesis on the neuroprotective action of this post-transcriptional factor in the injured brain. We observed that the upregulation of miR-29 associated with improved motor recovery is in line with previous studies of miR-29 in stroke animal models showing improved outcomes upon augmented miRNA levels (Khanna et al., 2013, Wang et al., 2015).

Materials and Methods

1 Mice

All procedures involving mice were performed in accordance with the rules of the Italian Minister of Health. Mice were housed in clear plastic cages under a 12 h light/dark cycle and were given ad libitum access to water and food. We used a transgenic mouse line, C57BL/6J-Tg(Thy1GCaMP6f)GP5.17Dkim/J, from Jackson Laboratories (Bar Harbor, Maine USA). Each group contained comparable numbers of male and female mice, and the age of mice was consistent between the groups (Sham n=4; Stroke n=4; Optostim n=4; Robot= 3; Optostim+Robot (OR) n= 4).

2 Surgical procedures

2.1 Channelrhodopsin 2 injection

All surgical procedures were performed under isoflurane anesthesia (3% induction, 1.5% maintenence, in 1L/min oxygen). Body temperature was maintained at 37°C and mice were monitored using respiratory rate and toe pinch throughout the procedure. The animals were placed into a stereotaxic apparatus (Stoelting, Wheat Lane, Wood Dale, IL 60191). The skin over the skull was cut and the periosteum was removed with a blade. We used a dental drill to create a small craniotomy over somatosensory cortex, which was identified by stereotaxic coordinates. ChR2 injections were performed during the same surgical session in which the photothrombotic lesions were created. We injected 0.5 μL of AAV9-CaMKII-ChR2-mCherry ($2.48*10^{13}$ GC/mL) 600 μm deep inside the cortex at (i) -0.75 anteroposterior, +1.75 mediolateral. In Stroke, Optostim, Robot and OR mice this surgery was followed by the stroke induction. Robot mice were injected with ChR2 though the animals will not optogenetically stimulated. We applied this precaution not to underestimate a possible effect of LED excitation of Chr2 expressing neurons during calcium imaging. In Sham mice a cover glass and an aluminum head- post were attached to the skull using transparent dental cement (Super Bond, C&S), then the animals were placed in a heated cage (temperature 38°) until they fully recovered.

2.2 Photothrombotic lesion

The primary motor cortex (M1) was identified (stereotaxic coordinates +1,75 lateral, -0.5 rostral from bregma). Five minutes after intraperitoneal injection of Rose Bengal (0.2 ml, 10 mg/ml solution in Phosphate Buffer Saline (PBS); Sigma Aldrich, St. Louis, Missouri, USA), white light from an LED lamp (CL 6000 LED, Carl Zeiss Microscopy, Oberkochen, Germany) was focused with a 20X objective (EC Plan Neofluar NA 0.5, Carl Zeiss Microscopy, Oberkochen, Germany) and used to illuminate the M1 for 15 min to induce unilateral stroke in the right hemisphere. The CTRL animals are not subjected to photothrombosis. A cover glass and an aluminum head- post were attached to the skull using transparent dental cement (Super Bond, C&S). We waited at least 4-5 days after the surgery for the mice to recover before the first imaging session. After the last imaging session, all animals were perfused first with 20-30 mL of 0.01 M PBS (pH 7.6) and then with 150 mL of Paraformaldehyde 4% (PFA, Aldrich, St. Louis, Missouri, USA).

3 Robotic rehabilitation

Mice were allowed to become accustomed to the apparatus before the first imaging session so that they became acquainted with the new environment. The animals were trained by means of the M- Platform, which is a robotic system that allows mice to perform a retraction movement of their left forelimb (Spalletti et al., 2014). Briefly, the M-Platform is composed of a linear actuator, a 6-axis load cell, a precision linear slide with an adjustable friction system and a custom-designed handle that is fastened to the left wrist of the mouse. The handle is screwed onto the load cell, which permits a complete transfer of the forces applied by the animal to the sensor during the training session. Each training session was divided into “trials” that were repeated sequentially and consisted of 5 consecutive steps. First, the linear actuator moved the handle forward and extended the mouse left forelimb by 10 mm (full upper extremity extension). Next, the actuator quickly decoupled from the slide and a tone lasting 0.5 s informed the mouse that it should initiate the task. If the animal was able to overcome the static friction (approximately 0.2 N), it voluntarily pulled the handle back by retracting its forelimb (i.e. forelimb flexion back to the starting position). Upon successful completion of the

task, a second tone that lasted 1 sec was emitted and the animal was given access to a liquid reward, i.e. 10 µl of sweetened condensed milk, before starting a new cycle. To detect the movement of the wrist of the animal in the low-light condition of the experiment, an infrared (IR) emitter was placed on the linear slide, and rigidly connected to the load cell and thus to the animal's wrist. Slide displacement was recorded by an IR camera (EXIS WEBCAM #17003, Trust) that was placed perpendicular to the antero-posterior axis of the movement. Position and speed signals were subsequently extracted from the video recordings and synchronized with the force signals recorded by the load cell (sampling frequency = 100 Hz).

To realize the adjustment of the friction of the device during the calibration a rigid component connect the actuator with the slide. This component mimics the effect of the retraction movements performed by the animal, reproducing the applied forces in direction and point of application.

All groups performed at least one week (5 sessions) of daily training, starting 26 days after injury for Sham and Optostim mice, 5 days after stroke for Robot and Optostim+Robot groups and after the surgery for Ctrl animal.

4 Optogenetic stimulation

Awake head fixed mice were place under the wide field microscope to perform daily session of optogenetic stimulation. A blue 473 nm laser is used to deliver 5 Hz, 10ms light pulses with a power range of 0.2-0.8 mW. The laser power is adjusted during the rehabilitation period according to the increment of the transfected area and set at a value lower than the one necessary to elicit movements in the affected forelimb. The system is provided with a random-access scanning head, developed using two orthogonally-mounted acousto-optical deflectors (DTSXY400, AA Opto-Electronic). The acousto-optic deflectors rapidly scan lines with a commutation time » 5 µs between a line and the next. After scanning the desired shape (in this case a cros) acousto-optic deflector returned to the initial position and repeated the cycle for the total illumination time. The stimulation protocol consists of 3 successive 30 s stimulation daily separated by 1 min rest intervals. All animals (Sham, Optostim and Optostim+Robot), except for Ctrl and Robot-F groups, were stimulated every day for four weeks, five days after photothrombosis.

5 Schallert Cylinder Test

Mice were placed in a Plexiglas cylinder (7,5 cm diameter, 16 cm height) and recorded for five minutes by a webcam placed below the cylinder, after 2 minutes of acclimatization. Videos were analyzed frame by frame and the spontaneous use of both forelimbs was assessed during exploration of the walls, by counting the number of contacts performed by the paws of the animal. For each wall exploration, the last paw that left and the first paw that contacted the wall or the ground were assessed. The experimenter was blind to the experimental group. In order to quantify forelimb-use asymmetry displayed by the animal, an Asymmetry index was computed, according to Lai et al. 2015 (Lai et al., 2015).

6 Wide-field fluorescence microscope

The custom-made wide-field imaging setup was equipped with two excitation sources allowing imaging of GCaMP6f fluorescence and light-stimulation of ChR2. For imaging of GCaMP6f fluorescence, a 505 nm LED (M505L3 Thorlabs, New Jersey, United States) light was deflected by a dichroic filter (DC FF 495-DI02

Semrock, Rochester, New York USA) on the objective (2.5x EC Plan Neofluar, NA 0.085, Carl Zeiss Microscopy, Oberkochen, Germany). A 3D motorized platform (M-229 for xy plane, M-126 for z-axis movement; Physik Instrumente, Karlsruhe, Germany) allowed sample displacement. The fluorescence signal was selected by a band pass filter (525/50 Semrock, Rochester, New York USA). Then a 20X objective (LD Plan Neofluar, 20x/0.4 M27, Carl Zeiss Microscopy, Oberkochen, Germany) was used to demagnify the image onto a 100X100 pxl2 area of the sCMOS camera sensor (OrcaFLASH 4.0, Hamamatsu Photonics, NJ, USA). Images (5.2 x 5.2 mm^2, pixel size 52 µm) were acquired at 25 Hz.

To perform optogenetic stimulation of ChR2, a 473 nm continuous wavelength (CW) laser (OBIS 473nm LX 75mW, Coherent, Santa Clara, California, United States) was overlaid on the imaging path using a second dichroic beam splitter (FF484-Fdi01-25x36, Semrock, Rochester, New York USA). The system has a random-access scanning head with two orthogonally-mounted acousto-optical deflectors (DTSXY400, AA Opto-Electronic, Orsay France).

7 Image analysis

Analysis of the fluorescent image stacks were previously reported in Allegra et al. 2019. Briefly, image stacks were registered manually and synchronized to the force data. For all stacks the ΔF/F_0 was computed and 3 seconds time windows were extracted (0.4 sec before and 2.6 sec after) around force peaks that resulted in the movement of the slide. A summed intensity projection (SIP) was then obtained by summing all the time windows in a day of training, this SIP was then thresholded to its median plus one standard deviation to generate a binary image per day. Binary images for each day of a week of training were then superimposed and the common area that was activated in at least 3 days was selected as the region of interest used to extract calcium signal parameters for subsequent analyses. This region of interest was the used to extract the Peak amplitude and Slope of the ΔF/F_0 for each week of training for each animal (for a formal definition of these measures see Allegra et al. 2019).

8 Force analysis

To quantify the behavior of each animal on the platform we analyzed the exerted by the mouse during the retraction phase. For each peak associated with the movement of the slide we extracted four parameters: 1) Peak amplitude as its max value; 2) Peak width (full half width maximum) as the width of the peak at half the peak amplitude; 3) Peak area as area of the force signal during its peak width and 4) the time to target as the time between the start of the trial and the peak associated with the last movement of the slide in the trial.

9 Immunohistochemical analysis

For immunohistochemical analysis of plasticity markers, animals were transcardially perfused with 4% paraformaldehyde. Brains were cut using a vibrating-blade microtome (Leica, Germany) to obtain 100 µm thick coronal sections that were used for immunostaining of NeuN (1:200, Millipore, Germany), Parvalbumin (1:500, Abcam, United Kingdom) and GAP 43 (1:600, Abcam, United Kingdom). The number of Parvalbumin- and GAP43- positive neurons was analyzed using a confocal fluorescence microscope (Nikon Eclipse TE 300, Tokyo, Japan) with a Nikon Plan EPO 60x objective (NA 1.4, oil immersion Nikon, Tokyo, Japan), acquiring 212,13 µm wide images in the periinfarct cortex. Three sections per animal were analyzed.

To evaluate the extension of the lesion we use a 10x objective (C-Apochromat, 0.45 NA, Carl Zeiss Microscopy, Oberkochen, Germany field of view 1.3 mm). Then, for each animal was calculated by summing up all damaged areas and multiplying the number by section thickness and by 3 (the spacing factor). A total volume in mm^3 is given as the mean ± standard error of all analyzed animals (n=15).

Lai, S., Panarese, A., Spalletti, C., Alia, C., Ghionzoli, A., Caleo, M., and Micera, S. (2015). Quantitative kinematic characterization of reaching impairments in mice after a stroke. Neurorehabil Neural Repair *29*, 382-392.

Acknowledgments

We thank K. Deisseroth for opsin plasmids. This project has received funding from the H2020 EXCELLENT SCIENCE - European Research Council (ERC) under grant agreement 692943 BrainBIT. In addition, it was supported by the European Union's Horizon 2020 Research and Innovation Programme under Grant Agreements 785907 (HBP SGA2), and 654148 (Laserlab-Europe). Part of this work was performed within the framework of the Proof of Concept Studies for the ESFRI research infrastructure project Euro-BioImaging at the PCS facility LENS.

Author Contributions

E.C. and A.L.A.M. conceived the study. E.C. and A.L.A.M. performed experiments. E.C., A.S., G.d.V., M.P., F.C. and processed data. F.S.P., T.P. and S.M. obtained funding support. E.C. and A.L.A.M. wrote the paper. All authors approved the paper.

Declaration of Interests

The authors declare no competing interests.

References

Alia, C., Spalletti, C., Lai, S., Panarese, A., Lamola, G., Bertolucci, F., Vallone, F., Di Garbo, A., Chisari, C., Micera, S., *et al.* (2017). Neuroplastic Changes Following Brain Ischemia and their Contribution to Stroke Recovery: Novel Approaches in Neurorehabilitation. Front Cell Neurosci *11*, 76.

Allegra Mascaro, A.L., Conti, E., Lai, S., Di Giovanna, A.P., Spalletti, C., Alia, C., Panarese, A., Scaglione, A., Sacconi, L., Micera, S., *et al.* (2019). Combined Rehabilitation Promotes the Recovery of Structural and Functional Features of Healthy Neuronal Networks after Stroke. Cell Rep *28*, 3474-3485 e3476.

Balasubramanian, S., Klein, J., and Burdet, E. (2010). Robot-assisted rehabilitation of hand function. Curr Opin Neurol *23*, 661-670.

Balbi, M., Vanni, M.P., Vega, M.J., Silasi, G., Sekino, Y., Boyd, J.D., LeDue, J.M., and Murphy, T.H. (2018). Longitudinal monitoring of mesoscopic cortical activity in a mouse model of microinfarcts reveals dissociations with behavioral and motor function. J Cereb Blood Flow Metab, 271678X18763428.

Biernaskie, J., and Corbett, D. (2001). Enriched rehabilitative training promotes improved forelimb motor function and enhanced dendritic growth after focal ischemic injury. J Neurosci *21*, 5272-5280.

Boyden, E.S., Zhang, F., Bamberg, E., Nagel, G., and Deisseroth, K. (2005). Millisecond-timescale, genetically targeted optical control of neural activity. Nat Neurosci *8*, 1263-1268.

Buetefisch, C.M. (2015). Role of the Contralesional Hemisphere in Post-Stroke Recovery of Upper Extremity Motor Function. Front Neurol *6*, 214.

Butefisch, C.M. (2006). Neurobiological bases of rehabilitation. Neurol Sci *27 Suppl 1*, S18-23.

Butefisch, C.M., Wessling, M., Netz, J., Seitz, R.J., and Homberg, V. (2008). Relationship between interhemispheric inhibition and motor cortex excitability in subacute stroke patients. Neurorehabil Neural Repair *22*, 4-21.

Carmichael, S.T. (2003). Plasticity of cortical projections after stroke. Neuroscientist *9*, 64-75.

Carmichael, S.T., Archibeque, I., Luke, L., Nolan, T., Momiy, J., and Li, S. (2005). Growth-associated gene expression after stroke: evidence for a growth-promoting region in peri-infarct cortex. Exp Neurol *193*, 291-311.

Cheng, M.Y., Wang, E.H., Woodson, W.J., Wang, S., Sun, G., Lee, A.G., Arac, A., Fenno, L.E., Deisseroth, K., and Steinberg, G.K. (2014). Optogenetic neuronal stimulation promotes functional recovery after stroke. Proc Natl Acad Sci U S A *111*, 12913-12918.

Conti, E., Allegra Mascaro, A.L., and Pavone, F.S. (2019). Large Scale Double-Path Illumination System with Split Field of View for the All-Optical Study of Inter-and Intra-Hemispheric Functional Connectivity on Mice. Methods Protoc *2*.

Dancause, N., and Nudo, R.J. (2011). Shaping plasticity to enhance recovery after injury. Prog Brain Res *192*, 273-295.

Dong, Y., Winstein, C.J., Albistegui-DuBois, R., and Dobkin, B.H. (2007). Evolution of FMRI activation in the perilesional primary motor cortex and cerebellum with rehabilitation training-related motor gains after stroke: a pilot study. Neurorehabil Neural Repair *21*, 412-428.

Hogan, N., and Krebs, H.I. (2011). Physically interactive robotic technology for neuromotor rehabilitation. Prog Brain Res *192*, 59-68.

Iwai, M., Stetler, R.A., Xing, J., Hu, X., Gao, Y., Zhang, W., Chen, J., and Cao, G. (2010). Enhanced oligodendrogenesis and recovery of neurological function by erythropoietin after neonatal hypoxic/ischemic brain injury. Stroke *41*, 1032-1037.

Jaillard, A., Martin, C.D., Garambois, K., Lebas, J.F., and Hommel, M. (2005). Vicarious function within the human primary motor cortex? A longitudinal fMRI stroke study. Brain *128*, 1122-1138.

Jones, T.A., Chu, C.J., Grande, L.A., and Gregory, A.D. (1999). Motor skills training enhances lesion-induced structural plasticity in the motor cortex of adult rats. J Neurosci *19*, 10153-10163.

Lai, S., Panarese, A., Spalletti, C., Alia, C., Ghionzoli, A., Caleo, M., and Micera, S. (2015). Quantitative kinematic characterization of reaching impairments in mice after a stroke. Neurorehabil Neural Repair *29*, 382-392.

Li, N., Daie, K., Svoboda, K., and Druckmann, S. (2016). Robust neuronal dynamics in premotor cortex during motor planning. Nature *532*, 459-464.

Liepert, J., Graef, S., Uhde, I., Leidner, O., and Weiller, C. (2000). Training-induced changes of motor cortex representations in stroke patients. Acta Neurol Scand *101*, 321-326.

Murase, N., Duque, J., Mazzocchio, R., and Cohen, L.G. (2004). Influence of interhemispheric interactions on motor function in chronic stroke. Ann Neurol *55*, 400-409.

Murphy, T.H., and Corbett, D. (2009). Plasticity during stroke recovery: from synapse to behaviour. Nat Rev Neurosci *10*, 861-872.

Nudo, R.J., Wise, B.M., SiFuentes, F., and Milliken, G.W. (1996). Neural substrates for the effects of rehabilitative training on motor recovery after ischemic infarct. Science *272*, 1791-1794.

Sawaki, L., Butler, A.J., Leng, X., Wassenaar, P.A., Mohammad, Y.M., Blanton, S., Sathian, K., Nichols-Larsen, D.S., Wolf, S.L., Good, D.C., *et al.* (2008). Constraint-induced movement therapy results in increased motor map area in subjects 3 to 9 months after stroke. Neurorehabil Neural Repair *22*, 505-513.

Schwab, M.E. (2010). How hard is the CNS hardware? Nat Neurosci *13*, 1444-1446.

Shimizu, T., Hosaki, A., Hino, T., Sato, M., Komori, T., Hirai, S., and Rossini, P.M. (2002). Motor cortical disinhibition in the unaffected hemisphere after unilateral cortical stroke. Brain *125*, 1896-1907.

Siegel, J.S., Ramsey, L.E., Snyder, A.Z., Metcalf, N.V., Chacko, R.V., Weinberger, K., Baldassarre, A., Hacker, C.D., Shulman, G.L., and Corbetta, M. (2016). Disruptions of network connectivity predict impairment in multiple behavioral domains after stroke. Proc Natl Acad Sci U S A *113*, E4367-4376.

Siegel, J.S., Seitzman, B.A., Ramsey, L.E., Ortega, M., Gordon, E.M., Dosenbach, N.U.F., Petersen, S.E., Shulman, G.L., and Corbetta, M. (2018). Re-emergence of modular brain networks in stroke recovery. Cortex *101*, 44-59.

Spalletti, C., Alia, C., Lai, S., Panarese, A., Conti, S., Micera, S., and Caleo, M. (2017). Combining robotic training and inactivation of the healthy hemisphere restores pre-stroke motor patterns in mice. Elife *6*.

Spalletti, C., Lai, S., Mainardi, M., Panarese, A., Ghionzoli, A., Alia, C., Gianfranceschi, L., Chisari, C., Micera, S., and Caleo, M. (2014). A robotic system for quantitative assessment and poststroke training of forelimb retraction in mice. Neurorehabil Neural Repair *28*, 188-196.

Straudi, S., Martinuzzi, C., Baroni, A., Benedetti, M.G., Foti, C., Sabbagh Charabati, A., Pavarelli, C., and Basaglia, N. (2016). Monitoring Step Activity During Task-Oriented Circuit Training in High-Functioning Chronic Stroke Survivors: A Proof-of-Concept Feasibility Study. Ann Rehabil Med *40*, 989-997.

Takatsuru, Y., Fukumoto, D., Yoshitomo, M., Nemoto, T., Tsukada, H., and Nabekura, J. (2009). Neuronal circuit remodeling in the contralateral cortical hemisphere during functional recovery from cerebral infarction. J Neurosci *29*, 10081-10086.

Tennant, K.A., Taylor, S.L., White, E.R., and Brown, C.E. (2017). Optogenetic rewiring of thalamocortical circuits to restore function in the stroke injured brain. Nat Commun *8*, 15879.

Vallone, F., Lai, S., Spalletti, C., Panarese, A., Alia, C., Micera, S., Caleo, M., and Di Garbo, A. (2016). Post-Stroke Longitudinal Alterations of Inter-Hemispheric Correlation and Hemispheric Dominance in Mouse Pre-Motor Cortex. PLoS One *11*, e0146858.

Volz, L.J., Vollmer, M., Michely, J., Fink, G.R., Rothwell, J.C., and Grefkes, C. (2017). Time-dependent functional role of the contralesional motor cortex after stroke. Neuroimage Clin *16*, 165-174.

Yizhar, O., Fenno, L.E., Davidson, T.J., Mogri, M., and Deisseroth, K. (2011). Optogenetics in neural systems. Neuron *71*, 9-34.

Zeiler, S.R., and Krakauer, J.W. (2013). The interaction between training and plasticity in the poststroke brain. Curr Opin Neurol *26*, 609-616.

Zhao, Y., and Rempe, D.A. (2010). Targeting astrocytes for stroke therapy. Neurotherapeutics *7*, 439-451.

Supplementary Materials

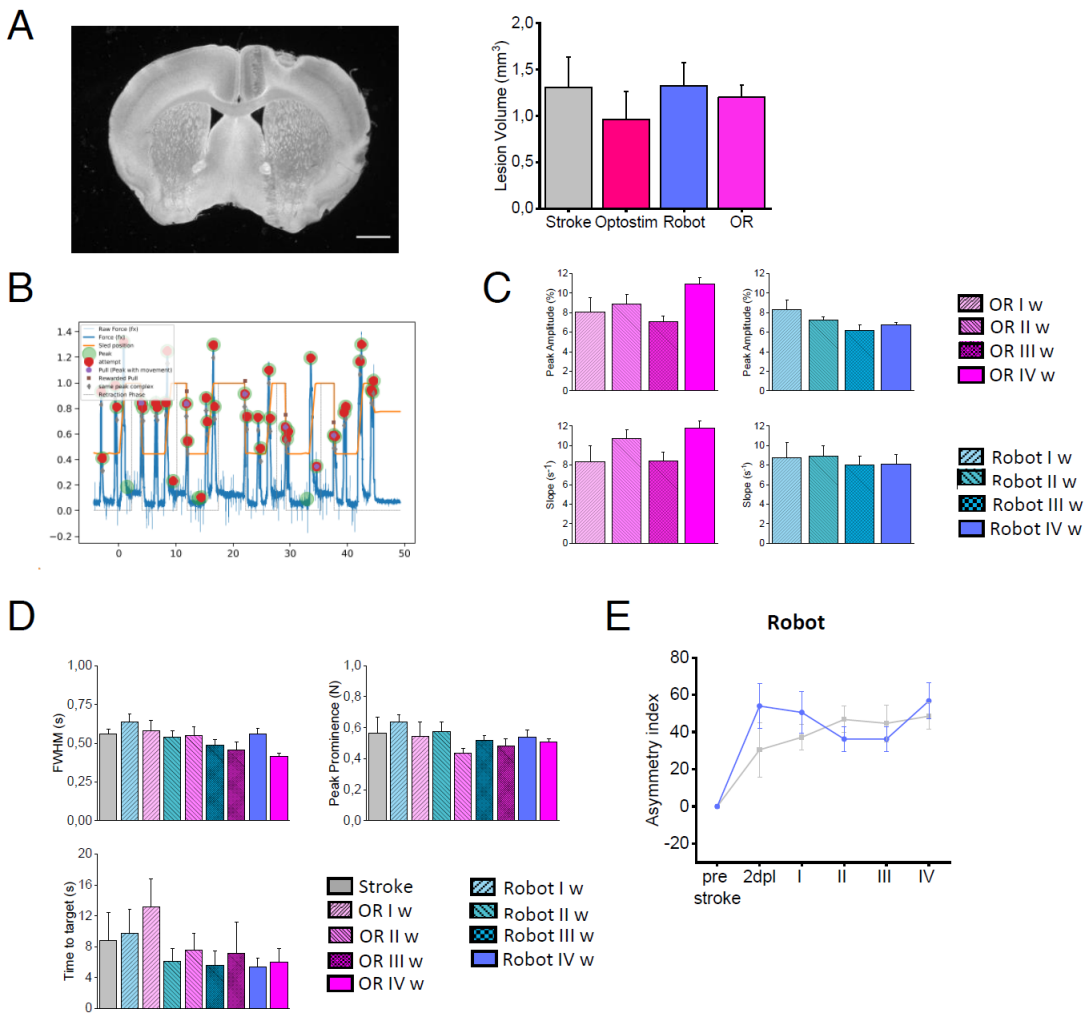

Supplementary Figure 1. Optogenetic stimulation of peri-infarct area: (A) Coronal section of a mouse brain 30 days after photothrombosis, 1 mm scale bar. The right panel shows the quantification of the lesioned area in the experimental groups. (B) Force trace (in blue) registered by the load cell of M-Platform during a training session. The force analysis showed the sled position during the session (in orange), the attempts to reach the home position (red spot), the force peaks associated to movement (violet spot) and the pulling associated with reward (bordeaux square). (C) Longitudinal analysis of cortical activation profiles over the four weeks for Robot (Amplitude: Iw= 8.3 ± 1.0; IIw= 7.3± 0.3; III= 6.1± 0.6; IV= 6.7 ±0.3; Slope: Iw= 8.8± 1.5; IIw= 8.9 ± 1.0; III= 8.0 ± 0.9; IV= 8.1 ± 0.9) and OR groups (Amplitude: Iw=8.1 ± 1,4; IIw= 8.9 ± 0.9; III= 7.1 ± 0.5; IV= 10.9 ± 0.7; Slope: Iw= 8.3 ± 1.6; IIw= 10.7 ± 0.9; III= 8.4 ± 0.9; IV= 11,8 ± 0.7). (D) Force analysis during pulling task. Left upper panel shows the Full Width Half Maximum of the force peak (Stroke= 0,56 ± 0,03; Robot_Iw= 0,64 ± 0,05; OR_Iweek= 0,58 ± 0,07; Robot_IIw= 0,54 ± 0,04; OR_IIweek= 0,55 ± 0,06; Robot_IIIw= 0,49 ± 0,03; OR_IIIweek= 0,45 ± 0,05; Robot_IVw= 0,56 ± 0,04; OR_IVweek= 0,42 ± 0,02; t-test: pStroke-OR_IVweek= 0,03). Right upper panel show the Peak Prominence (Stroke= 0,56 ± 0,1; Robot_Iw= 0,63 ± 0,05; OR_Iweek= 0,54 ± 0,18; Robot_IIw= 0,58 ± 0,06; OR_IIweek= 0,43 ± 0,06; Robot_IIIw= 0,52 ± 0,03; OR_IIIweek= 0,48 ± 0,04; Robot_IVw= 0,54 ± 0,04; OR_IVweek= 0,5 ± 0,04) and the lower panel shows the Time to Target (Stroke= 8,8 ± 3,6; Robot_Iw= 9,7 ± 3,2; OR_Iweek= 13,2 ± 3,6;

Robot_IIw= 6,1 ± 1,6; OR_IIweek= 7,6 ± 2,1; Robot_IIIw= 5,6 ± 1,8; OR_IIIweek= 7,1 ± 4,1; Robot_IVw= 5,4 ± 1,2; OR_IVweek= 6,0± 1,8). (E) Asymmetry index analysis of Robot group (in blue) compared to non-rehabilitated animals (Stroke group in grey).

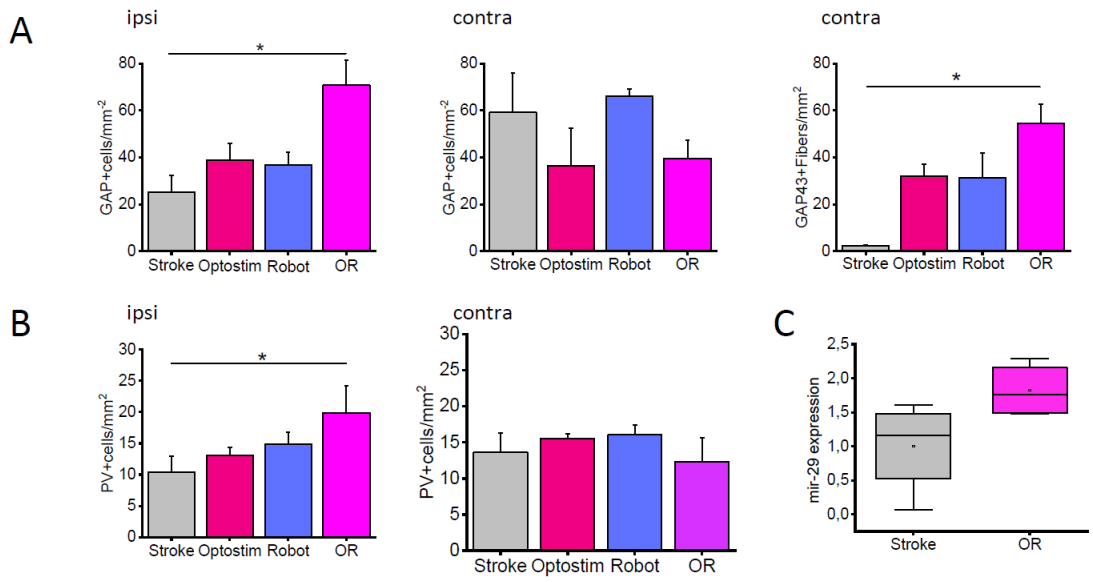

Supplementary Figure 2. (A) Immunohistochemical analysis of the ipsilesional (left panel) and contralesional hemisphere of GAP43+ cells for the experimental groups. Left panel shows the quantification of GAP43+ cells in the experimental groups in the peri-infarct area (Stroke= 25,0 ± 7,2; Optostim= 38,7 ± 7,2; Robot= 36,7 ± 5,6; OR= 70,7 ± 10,7; one-way ANOVA followed by Fisher's test: pStroke-OR= 0,011). Middle panel shows the quantification of GAP43+ cells in the contralesional hemisphere (Stroke= 59,1 ± 16,9; Optostim= 36,5 ± 16,1; Robot= 66,1 ± 3,2; OR= 70,7 ± 10,7). Right panel shows the quantification of GAP43+ fibers in the experimental groups in the ipsilesional area (Stroke= 2,4 ± 0,4; Optostim= 31,8 ± 5,4; Robot= 31,2 ± 10,7; OR= 54,4 ± 8,3; one-way ANOVA followed by Bonferroni's test: pStroke-OR= 0,006). (B) Immunohistochemical analysis of the ipsilesional (left panel) and contralesional hemisphere of PV positive cells for the experimental groups. Left panel shows the quantification of PV+ cells in the experimental groups in the peri-infarct area (Stroke= 19,7 ± 5,0; Optostim= 24,7 ± 2,5; Robot= 28,3 ± 3,6; OR= 37,7 ± 8,3; one-way ANOVA followed by Fisher's test: pStroke-OR= 0,04). Right panel show the quantification of PV+ cells in the contralesional hemisphere (Stroke= 13,6 ± 2,6; Optostim= 15,5 ±0, 7; Robot= 16,0 ± 1,4; OR= 12,2 ± 3,3). (C) Quantification of the ipsilesional expression of miR29 in Stroke and OR groups (Stroke= 1 ± 0,3 ; OR= 1,8 ± 0,2; pStroke-OR= 0,09).